

PAPER

Antenna Gain Measurements in the Presence of Unwanted Multipath Signals Using a Superresolution Technique

Hiroyoshi YAMADA[†], Yasutaka OGAWA[†] and Kiyohiko ITOH[†], *Members*

SUMMARY A superresolution technique is considered for use in antenna gain measurements. A modification of the MUSIC algorithm⁽¹⁾ is employed to resolve incident signals separately in the time domain. The modification involves pre-processing the received data using a spatial scheme⁽²⁾⁻⁽⁴⁾ prior to applying the MUSIC algorithm. Interference rejection in the antenna measurements using the fast Fourier transform (FFT) based techniques have been realized by a recently developed vector network analyzer, and its availability has been reported in the literature.^{(5),(6)} However, response resolution in the time domain of these conventional techniques is limited by the antenna bandwidth. The MUSIC algorithm has the advantage of being able to eliminate unwanted responses when performing antenna measurements in situations where the antenna bandwidth is too narrow to support FFT based techniques. In this paper, experimental results of antenna gain measurements in a multipath environment show the accuracy and resolving power of this technique.

key words: antenna gain measurements, multipath environments, MUSIC algorithm, spatial smoothing preprocessing

1. Introduction

In the measurements of gain and radiation pattern for a large aperture antenna, a measurement system often must be constructed outdoors to achieve a far-field range. In this case, reflected signals from the ground and other objects often impinge on the antenna, disturbing measured data. High level test ranges, ground level test ranges, etc., that utilize spatial (physical) relationships among antennas and scatterers (e.g. ground and buildings), have been devised to reduce the effect of such unwanted responses. The ranges which cover the wide bandwidth and have flexibility in antenna positioning, may be difficult to realize in such a multipath environment, so that we must design the outdoor ranges to compensate for multipath interference in some limited frequency band and antenna position/height. In view of recent situations of land and buildings, it is becoming very difficult to achieve a good far-field range. A compact range is one of the promising methods for realizing a far-field range equivalently in a small space. However, establishment of antenna measurements in multipath

environments is meaningful for enhancement of the measurement accuracy in the existing far-field ranges, and for making design of the ranges flexible. It is often difficult, however, to achieve enough accuracy because of high operation frequency and/or narrow pass-bandwidth. Many improvements have been presented to enhance measurement accuracy.

A recently developed vector network analyzer provides time-domain processing based on the fast Fourier transform (FFT) algorithm. This algorithm can be utilized in swept frequency measurements to enhance the measurement accuracy even when there exist unwanted responses, that appear as ripples in the frequency domain, extraction of only desired response(s) can be done by gating in the time-domain presentation. Because the processing is mathematical, the measurement system hardly has physical restrictions compared with the measurement ranges stated above. Then, high measurement flexibility, in addition to the measurement accuracy, can be realized.^{(5),(6)}

However, desired (direct path) and unwanted (e.g. ground path) responses must be clearly separated in the time-domain presentation to apply the time-domain processing correctly. If the skirts of the responses are overlapped with each other, the time-domain gating cannot work properly, and a gating error occurs in the processed data. The response resolution of the inverse FFT (IFFT) essentially depends on the frequency bandwidth of obtained data. Also, outdoor wideband measurements are often not preferable because the wideband radiation may interfere with another radio system. In the antenna measurements, signal detection and interference rejection using the data within the operating frequency bandwidth are desired. Namely, high resolution time-domain estimation has been eagerly desired.

We propose to apply a superresolution technique to the antenna measurement data. Among various superresolution techniques, we adopt a MUSIC (MULTiple SIGNAL Classification) algorithm.⁽¹⁾ The other eigenstructure based superresolution techniques, for example, MFBLP,⁽⁷⁾ ESPRIT,⁽⁸⁾ etc. are also applicable to the antenna measurements, because they are formulated for the same signal model as the MUSIC. The MUSIC algorithm has been widely studied, espe-

Manuscript received May 20, 1992.

Manuscript revised November 24, 1992.

[†] The authors are with the Faculty of Engineering, Hokkaido University, Sapporo-shi, 060 Japan.

cially for the direction finding problem, and then, we can say that the MUSIC is a representative superresolution technique among them. It is difficult to choose the best algorithm. Our goal in this paper is not to choose the most suitable technique for the antenna measurements. The results of the MUSIC reported here will be also a good reference when we adopt another eigenstructure based superresolution technique.

A spatial smoothing scheme⁽²⁾⁻⁽⁴⁾ must be carried out to the measured frequency-domain data before applying the MUSIC algorithm. This is because the received signals in this case are time invariant in contrast with the usual direction finding problem. We have reported the effectiveness of the algorithms for electromagnetic circuit measurements.⁽⁹⁾ In that paper, we showed that the MUSIC algorithm preprocessed by the spatial smoothing method has higher capability of resolving signals (discrete points of reflection) compared with the conventional FFT technique. Our main objectives in this paper are, first, to separate incident signals in the time domain using narrower frequency-domain antenna transmission data, then, to eliminate the effect of unwanted signal(s) in the frequency-domain presentation. We made a multipath environment model in a radio anechoic chamber, and demonstrated the high response resolution capability of the MUSIC algorithm. Measured values of the actual antenna gain in the multipath environment are also presented. The algorithm employed here is essentially the same as that described in Ref. (9). However, characteristics of the measured device (antenna) and measurement system have quite different features. For the circuit measurements as discussed in Ref. (9), the calibration sequence can be done before applying the

MUSIC. On the contrary, we must apply the method to raw data without calibration and extract the desired responses in the antenna measurements. These procedures are required for both the antenna under test and the reference antenna. Next, the response is calibrated. Strictly speaking, the MUSIC algorithm is derived to treat frequency independent signals. The antenna is in general a frequency dependent device. In spite of these inadequate conditions for the MUSIC algorithm, experimental results reported in this paper are accurate. This is because of the narrow bandwidth that the MUSIC needs.

The paper is organized as follows. First, we introduce the received signal model in the antenna transmission measurement, and formulate the problem in Sect. 2. In Sect. 3, we present a brief review of the algorithm in this problem. We present some experimental results to illustrate its resolution capability in Sect. 4. Gain estimation results are also shown. Section 5 contains conclusions.

2. Problem Formulation

We consider an antenna transmission measurement. An overview of this scheme is shown in Fig. 1(a). In this figure, we show only one reflected path (a ground path reflection). Generally, there often exist some reflected signals from buildings and so forth in addition to it. The formulation stated below can be straightforwardly expanded into such a complicated multipath environment.

Amplitude and phase of the received signal as a function of frequency can be obtained by measurement equipment such as a vector network analyzer. Using

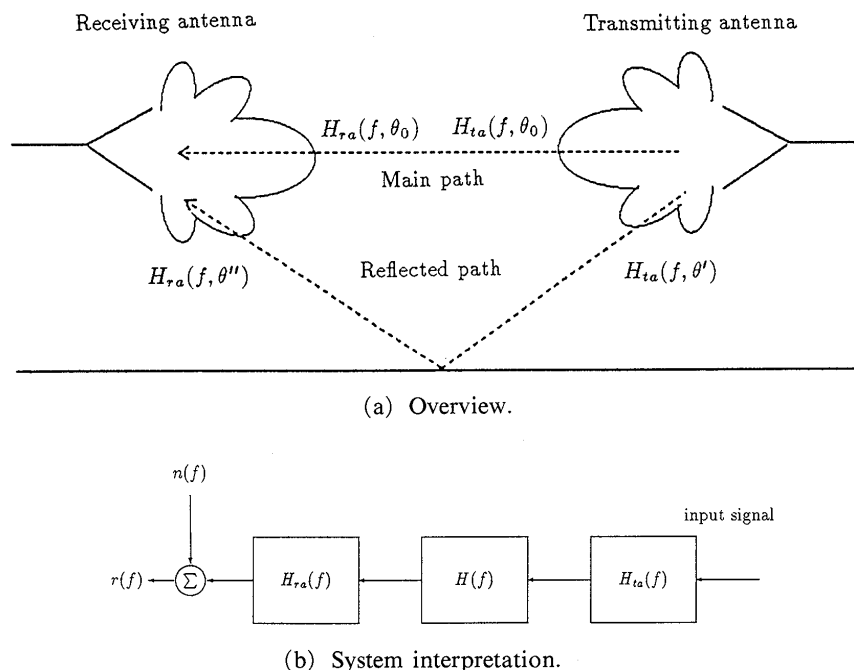


Fig. 1 Antenna measurement scheme.

the system interpretation, we can illustrate this scheme as Fig. 1(b). In this figure, $H_{ta}(f)$ and $H_{ra}(f)$ denote the transfer functions of transmitting and receiving antennas, respectively. In this paper, we assume that the receiving antenna is an antenna under test (AUT). Then, the measured data can be regarded as S_{21} data in the S -parameter expression. The transfer function $H(f)$ represents the propagation environment, and $n(f)$ denotes the additive noise. Then, the obtained frequency-domain data $r(f)$ are given by

$$r(f) = H_{ta}(f) \cdot H(f) \cdot H_{ra}(f) + n(f). \quad (1)$$

Referring to Fig. 1(a), we can rewrite Eq. (1) as

$$\begin{aligned} r(f) = & H_{ta}(f, \theta_0) H_{ra}(f, \theta_0) \rho_1 e^{-j2\pi f t_1} \\ & + H_{ta}(f, \theta') H_{ra}(f, \theta'') \rho_2 e^{-j2\pi f t_2} \\ & + n(f) \end{aligned} \quad (2)$$

where ρ_1 and ρ_2 denote transmission coefficients of the main and reflected path signals, respectively. They are assumed frequency invariant. Propagation delay time of each signal is expressed as t_1 and t_2 . Frequency dependence of the antenna transfer function can be neglected over a narrow frequency bandwidth. Then, Eq. (2) can be simplified as

$$r(f) = s_1 e^{-j2\pi f t_1} + s_2 e^{-j2\pi f t_2} + n(f) \quad (3)$$

where s_1 and s_2 denote the signal parameter of the main path and reflected path signals, respectively. The main path response is expressed as $s_1 e^{-j2\pi f t_1}$. Essentially Eq. (3) is the same form that we formulated for the electromagnetic circuit model.⁽⁹⁾ Then, we can say that the MUSIC algorithm can be applied for the antenna measurements discussed above.

When the duration of the antenna transient response is relatively long for assuming the frequency invariance of its transfer function but the interference signals can be clearly separated, the main path signal (desired response) often consists of several dominant signals. This may happen in measurements of large aperture antennas such as a reflector antenna. These signals are from the disk aperture, disk edges, and so forth (Ref. (10), Fig. 8.12). In such cases, the desired response can be expressed as

$$s_{main} = \sum_{i=1}^{d_0} s_i e^{-j2\pi f t_i} \quad (4)$$

where d_0 denotes the number of signals which construct the total main path response among the “ d ” incident signals. The antenna shape is always known previously so that we can distinguish between desired and undesired responses from their delay time information. When the swept frequency bandwidth is too narrow to distinguish phase changes from these d_0 signals, namely when $2\pi f t_i \cong 2\pi f t_j (i, j = 1 \cdots d_0)$ holds throughout the frequency band, then the model leads to Eq. (3).

From these results, L uniformly sampled

frequency-domain data ($r_i; i=1, 2, \dots, L$) can be written using the vector notation as follows:

$$r = As + n, \quad (5a)$$

$$r = [r_1, r_2, \dots, r_L]^T \quad (5b)$$

$$s = [s_1, s_2, \dots, s_d]^T, \quad (5c)$$

$$n = [n_1, n_2, \dots, n_L]^T, \quad (5d)$$

$$A = [a(t_1), a(t_2), \dots, a(t_d)], \quad (5e)$$

$$a(t_k) = [e^{-j2\pi f_1 t_k}, e^{-j2\pi f_2 t_k}, \dots, e^{-j2\pi f_L t_k}]^T, \quad (5f)$$

$$k = 1, 2, \dots, d.$$

Here, T denotes transpose. A given by Eq. (5e) is an $L \times d$ delay parameter matrix and $a(t_k)$ is called the “mode vector” of each signal.⁽¹⁾ In the above equations, we assume that there exist d incident signals for the general problem. Note that $d=2$ in a case of Fig. 1(a).

3. The MUSIC Algorithm in Antenna Measurements

The MUSIC algorithm⁽¹⁾ is the eigenstructure-based high resolution method that exploits certain structural properties of the data correlation matrix. From Eq. (5a), the data correlation matrix can now be expressed as

$$R = E[rr^H] = ASA^H + \sigma^2 I \quad (6)$$

where $E[\cdot]$ denotes the ensemble average, $S = E[ss^H]$ denotes the signal correlation matrix, I is the identity matrix, and H denotes complex conjugate transpose. σ^2 denotes the noise power. In a case of applying the MUSIC algorithm, the signal correlation matrix S must be nonsingular.⁽¹⁾ However, the signals of each propagation path ($s_i; i=1, 2, \dots, d$) express the transmission coefficients, then they are time invariant (complex) values.⁽⁹⁾ Consequently, the signal correlation matrix becomes singular. Therefore, decorrelation procedures are required to make it nonsingular. The decorrelation procedures considered here are called “spatial smoothing preprocessing” in the direction finding scheme. In this paper, we examine two techniques. One is the conventional spatial smoothing preprocessing (SSP),⁽²⁾ the other is the modified spatial smoothing preprocessing (MSSP).^{(3),(4)}

In each spatial smoothing preprocessing, the data vector r in Eq. (5a) is partitioned into M overlapped subarrays of size $N \geq d + 1$. Samples $\{r_1, r_2, \dots, r_N\}$ form the first subarray, the samples $\{r_2, r_3, \dots, r_{N+1}\}$ form the second subarray, etc. The SSP is a method which uses the average of the subarray’s data correlation matrices. That is,

$$R_{SSP} = \frac{1}{M} \cdot \sum_{k=1}^M R_k \quad (7)$$

where

$$\mathbf{R}_k = E[\mathbf{r}_k \mathbf{r}_k^H], \quad (8a)$$

$$\mathbf{r}_k = [r_k, r_{k+1}, \dots, r_{k+N-1}]^T. \quad (8b)$$

On the other hand, the MSSP is the method that uses \mathbf{R}_{MSSP} defined as

$$\mathbf{R}_{MSSP} = \frac{1}{2M} \sum_{k=1}^M (\mathbf{R}_k + \mathbf{J} \mathbf{R}_k^* \mathbf{J}) \quad (9)$$

where $*$ denotes complex conjugate, and \mathbf{J} is the $N \times N$ exchange matrix:

$$\mathbf{J} = \begin{bmatrix} 0 & 0 & \cdots & 0 & 1 \\ 0 & 0 & & 1 & 0 \\ \vdots & & \ddots & & \vdots \\ 0 & 1 & & 0 & 0 \\ 1 & 0 & \cdots & 0 & 0 \end{bmatrix}. \quad (10)$$

The MSSP is also called ‘‘forward-backward spatial smoothing.’’⁽⁴⁾ These spatial smoothing methods can destroy the signal coherence, that is, the signal correlation matrix in \mathbf{R}_{SSP} or \mathbf{R}_{MSSP} becomes nonsingular. Then, the MUSIC algorithm works properly with each preprocessed data correlation matrix (see Ref. (9) for the details).

The MUSIC algorithm uses the eigenstructure of the (preprocessed) data correlation matrix. The number of signals (d) is obtained by the number of eigenvalues of the correlation matrix which are larger than the noise power. Theoretically, the number of resolving signals with the SSP and the MSSP are equal to ‘ M ’ ($< N$) and ‘ $2M$ ’ ($< N$), respectively, when we apply the spatial smoothing scheme with ‘ M ’ subarrays to the data. Practically, however, the number of required subarrays to resolve ‘ d ’ signals is often greater than the theoretically required one because of the finiteness of the snapshots and modeling errors. They correspond to cross-spectral estimation errors, jammers, and wavefront distortions in the direction finding scheme reported in Ref. (11). The remaining ($N-d$) eigenvalues are equal to the noise power. Also, the delay time of each incident signal is acquired using the property that the eigenvectors corresponding to the minimum eigenvalues are orthogonal to the signal mode vectors. The following function is employed for testing the orthogonality in practice,^{(1),(9)}

$$P_{music}(t) = \frac{\mathbf{a}(t)^H \mathbf{a}(t)}{\mathbf{a}(t)^H \mathbf{E}_N \mathbf{E}_N^H \mathbf{a}(t)} \quad (11)$$

where \mathbf{E}_N is the $N \times (N-d)$ matrix whose columns are the $(N-d)$ eigenvectors corresponding to the minimum eigenvalues (noise power). When the delay time ‘ t ’ in Eq. (11) coincides with the delay time of the incident signal, the function has a sharp peak which diverges theoretically. Then, the delay param-

eters, t_i ; $i=1, 2, \dots, d$, can be estimated by the peak positions of $P_{music}(t)$. Note that the values of the peaks of $P_{music}(t)$ do not correspond to the incident signal power.

As we reported in Ref. (9), the decorrelation effect of the MSSP is superior to that of the SSP, hence the MUSIC algorithm preprocessed by the MSSP can resolve the signals with narrower frequency bandwidth data than that preprocessed by the SSP. We can say that the MSSP is more suitable than the SSP from the viewpoint of narrow-bandwidth measurement assumption described in the Sect. 2, in addition to the superior decorrelation capability.

After estimating the delay parameters, the individual transmission coefficient can be obtained by the following equation.⁽⁹⁾

$$\mathbf{s} = (\mathbf{A}^H \mathbf{A})^{-1} \mathbf{A}^H \mathbf{E}[\mathbf{r}]. \quad (12)$$

where $\mathbf{E}[\mathbf{r}]$ denotes the ensemble average. Practically, $\mathbf{E}[\mathbf{r}]$ is estimated using finite snapshots.⁽⁹⁾ Clearly, the main path signal, that we want to extract here, has the shortest delay time among the signals (see Fig. 1(a)). Then, s_1 becomes the desired signal response, when we arrange the delay time in increasing order ($t_1 < t_2 < \dots < t_d$). We can estimate the main path signal response s_1 by calculating Eq. (12).

Finally, we replace the AUT with a gain-standard horn antenna (STD), leaving all other conditions the same, and carry out the same procedures shown above. Then, the gain of the AUT can be obtained by comparing the results of the AUT and the STD. The gain of the AUT in decibels (G^{AUT})_{dB} is given by⁽¹⁰⁾

$$(G^{AUT})_{dB} = (G^{STD})_{dB} + 20 \log \left| \frac{s_1^{AUT}}{s_1^{STD}} \right| \quad (13)$$

where $(G^{STD})_{dB}$ is the gain of the STD, s_1^{AUT} is the transmission coefficient of the main path signal of the AUT and s_1^{STD} is that of the STD.

4. Experimental Results

In this section, we present experimental results of the antenna gain measurement. We placed a metal plate on the back wall in a radio anechoic chamber as shown in Fig. 2, and had an intentional reflection path. Clearly, there exist two dominant paths, and the reflected path signal was delayed from the main path signal by about 8 nsec. We employed a monopole antenna of the length about 2.4 cm as the AUT. A transmitting antenna we used is a linearly polarized broadband antenna covering the frequency range from 1 GHz to 18 GHz (EMCO model 3115). A horn antenna (NARDA model 644) was used for the STD. In this experiment, each antenna was vertically polarized so that the polarization was matched each other. The measurement system configuration is shown in Fig. 2. Our purpose in this experiment is to estimate

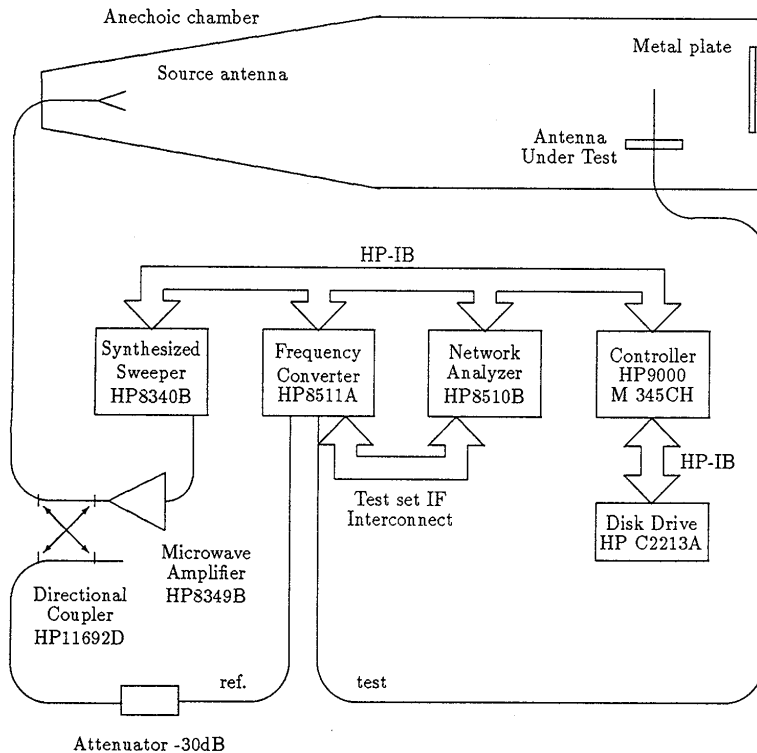


Fig. 2 Measurement system configuration.

the gain of the AUT in a "narrow" frequency bandwidth. First, we discuss the effect of the unwanted path signal in the frequency domain and time domain, then, show the results of the time-domain analyses using the IFFT and the MUSIC algorithm.

The measured frequency responses (magnitude) of the AUT are shown in Fig. 3. We see periodic ripples due to the interference by the reflected signal (the curve marked by "ungated response" in Fig. 3). A reciprocal of its period corresponds to the delay difference between the main path signal and reflected path one. If the obtained data frequency bandwidth is wide enough to detect the periodicity, we can estimate the isolated main path response. However, the estimation may fail if the frequency bandwidth is narrower than the period. Moreover, the detection becomes more difficult in a complicated multipath case. Then, time-domain techniques are required.

Figure 4 shows the time-domain responses calculated by the IFFT implemented in the HP8510B. As we see from this figure, the two signals cannot be detected by 100 MHz bandwidth data. The two peaks can be detected by 300 MHz bandwidth data. However, their estimated delay time can be biased since the skirts of each response are overlapped with each other, and then the gating technique may not work properly. Even if the precise delay time estimation can be done, direct application of Eq. (12) to the '300 MHz' bandwidth data cannot be assumed to be proper because the frequency dependence of each signal cannot be neglected in this frequency bandwidth generally. It is seen that we need about 1 GHz bandwidth data to resolve

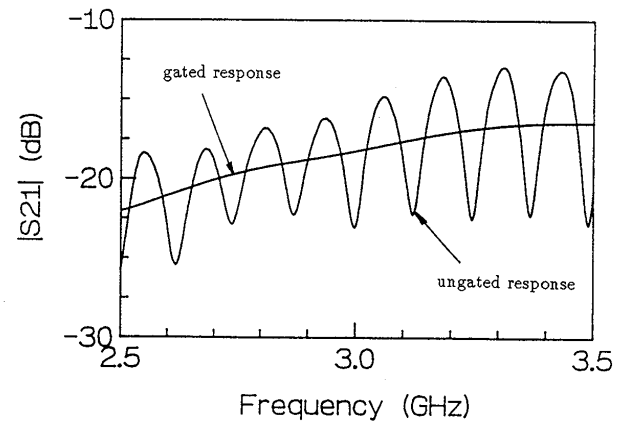


Fig. 3 Ungated and gated frequency-domain responses.

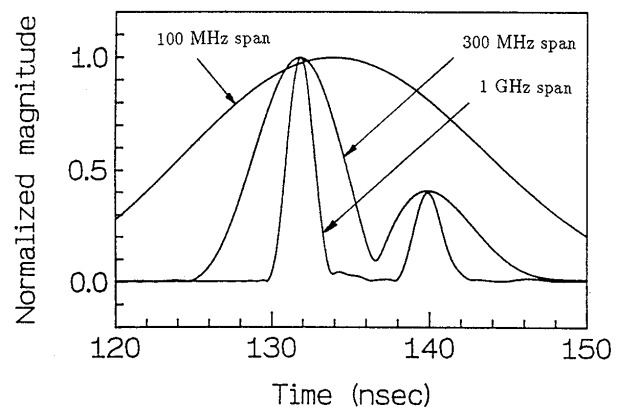
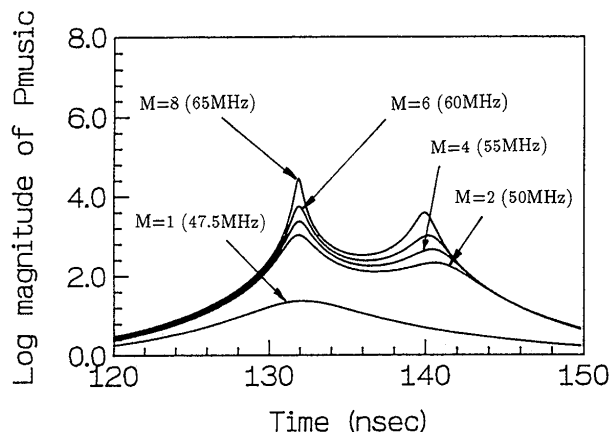


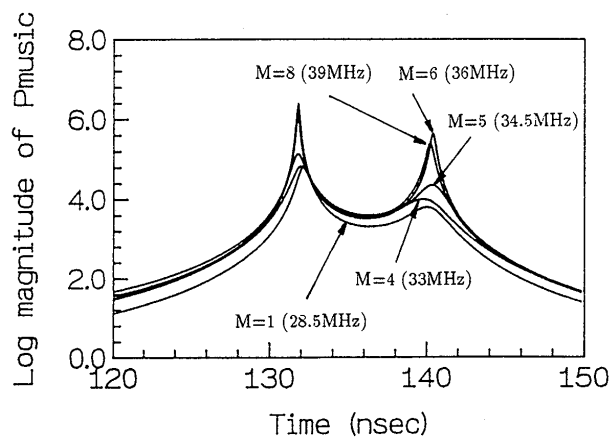
Fig. 4 Time-domain analysis using the IFFT. 1 GHz span: The measurement frequency band is from 2.5–3.5 GHz. 300 MHz span: The measurement frequency band is from 2.85–3.15 GHz. 100 MHz span: The measurement frequency band is from 2.95–3.05 GHz.

them completely, and the gating technique can be properly applied for the time-domain extraction in this case. The response processed by the time-domain gating is also shown in Fig. 3 (the curve marked by "gated response"). We may see that the magnitude error in the raw data (ungated response) is about 5 dB at 3.0 GHz. This is very large. The time-domain technique based on the Fourier transform is useful as shown above. Though it has no restrictions on the signal model, its response resolution depends on the frequency bandwidth. Then, it cannot be applied properly when the pass-bandwidth of the AUT is narrow.

Now, we show the results of the MUSIC algorithm. Figures 5(a) and (b) show the results of the MUSIC algorithm preprocessed by the SSP (MUSIC-SSP), and those by the MSSP (MUSIC-MSSP), respectively. 50 snapshots were used for estimation of R_k in Eq. (8a). Although a great number of snapshots are desired for the precise estimation of R_k , they will be limited by the allowable measurement time in practice. In the estimation using the MUSIC algorithm, the



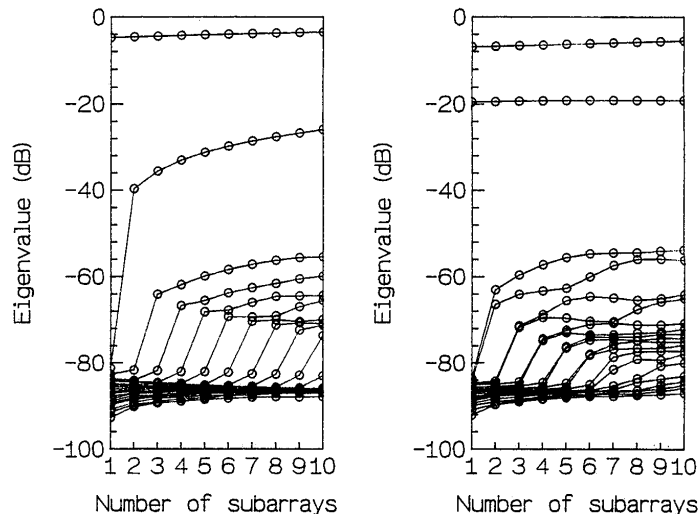
(a) The MUSIC-SSP. $N=20$, $f_1=3.0$ GHz, $\Delta f=2.5$ MHz.



(b) The MUSIC-MSSP. $N=20$, $f_1=3.0$ GHz, $\Delta f=1.5$ MHz.

Fig. 5 Time-domain analysis using the MUSIC algorithm. The value in the parenthesis () denotes the required frequency bandwidth.

lowest frequency of the data was fixed at 3.0 GHz ($f_1=3.0$ GHz). N must be larger than the number of received signals (d), then, we chose $N=20$, which is large enough in this case. Eigenvalue distribution in each analysis as a function of the smoothing index (M) is shown in Figs. 6(a) and (b). Two dominant eigenvalues are resolved in each analysis, then we chose the dimension of the signal subspace as two. Noise power can be estimated to be about -85 dB from the minimum eigenvalues. If we do not have any prior information on the number of incident signals, we should apply the MUSIC with some parameters (N , M , Δf), and then determine the number of dominant signals by the eigenvalue distributions. The sampling frequency period (Δf) must be chosen so as not to cause aliasing. The sampling frequency period in the MUSIC-SSP in Fig. 5(a) was 2.5 MHz, which covers the time span of about 400 nsec. Time span of about 667 nsec was covered by the sampling frequency period of 1.5 MHz used in the MUSIC-MSSP case (Fig. 5(b)). The main path response appears in the



(a) The MUSIC-SSP.
 $N=20$, $f_1=3.0$ GHz,
 $\Delta f=2.5$ MHz.

(b) The MUSIC-MSSP.
 $N=20$, $f_1=3.0$ GHz,
 $\Delta f=1.5$ MHz.

Fig. 6 Eigenvalues in each analysis as a function of the number of subarrays.

time-domain presentation at about 132 nsec. Then, we can say that the covered area is wide enough for each analysis in this experiment, even if there exist long delayed signals. The number of subarrays is marked by ' M ' in Figs. 5(a) and (b), and the required frequency bandwidth is also shown in the parenthesis. As we see from Fig. 5(a), the MUSIC algorithm cannot work properly when $M=1$. No decorrelation preprocessing is performed in this case, namely, the signals are completely coherent (see also Fig. 6(a)). As the number of subarrays increases, the correlation between the signals is decreased more effectively, then the eigenvalues corresponding to the incident signals can be clearly separated from others. Furthermore, the corresponding peaks in $P_{music}(t)$ become sharp. Then, we can say that the two peaks are successfully resolved by about 60 MHz bandwidth data in Fig. 5(a). As stated in the preceding section, the MSSP has better decorrelation performance than the SSP also in the antenna measurements. Consequently, the MUSIC-MSSP can realize the detection of signals by narrower frequency bandwidth data than the MUSIC-SSP. The frequency bandwidth can be reduced to only about 35 MHz for the MUSIC-MSSP as shown in Fig. 5(b).

The number of eigenvalues greater than the noise power (about -85 dB) is the number of resolvable signals as we mentioned previously. However, the number of the detected signals in each preprocessing scheme is not increased, even when we evaluate the function $P_{music}(t)$ assuming that there exist more than two signal eigenvalues. The cause that the eigenvalues appear around -60 dB is conjectured that there exist more than two signals but the power of them is too small for the MUSIC to resolve them using such

narrow-band data. In fact, more than two signals can be detected when we apply the MUSIC for wide-band data as shown in Fig. 7. We see that those detected peaks by the MUSIC coincide with those by the IFFT (3 GHz) to some extent. These signals are considered to be the reflected ones from the wall of the chamber as a clutter, and they are below both of the two dominant signals by more than 30 dB. Then, it can be considered that errors of the estimated signal parameters (also gain) due to these residual signals are negligible practically. Though the eigenvalue shown in Figs. 6(a) and (b), is not proportional to each signal power precisely, the eigenvalue distribution will be helpful to recognize the number of dominant signals.

If the delay time of each dominant signal can be correctly resolved in a narrow frequency bandwidth, we can obtain the signal parameters ($s_i; i=1, 2$) using Eq. (12). The time-domain gating technique, previously shown, requires the frequency bandwidth of about 1 GHz. Apparently, as shown in Fig. 4, we

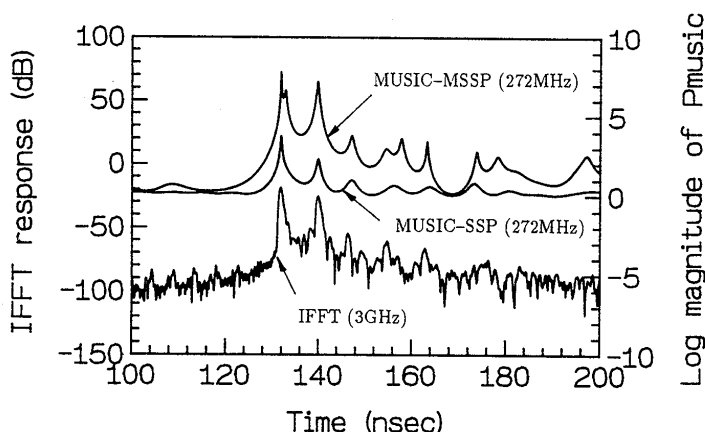


Fig. 7 Time-domain analysis with wide-band data. IFFT: The measurement frequency band is from 2-5 GHz. MUSIC-SSP: $f_i=3.0$ GHz, $\Delta f=4$ MHz, $N=50$, $M=20$, $d=20$. MUSIC-MSSP: $f_i=3.0$ GHz, $\Delta f=4$ MHz, $N=50$, $M=20$, $d=40$. The value in the parenthesis () denotes the required frequency bandwidth.

cannot even recognize the existence of two signals by the FFT technique when the frequency bandwidth is narrower than 100 MHz. On the other hand, when we employ the MUSIC-SSP, it needs only about 60 MHz bandwidth data for the detection. Furthermore, only 35 MHz bandwidth is enough for the interference rejection with the MUSIC-MSSP. The frequency bandwidth is almost 1/29 of that required by the FFT and the gating (FFT-GATE) techniques.

Next, we replaced the AUT with the STD. The reflected signal from the metal plate hardly disturbed this measurement because of the high front-to-back ratio of the STD. Namely, dominant reflected signals were not observed by either the IFFT or the MUSIC. The estimation using the MUSIC method was performed with the same parameters ($N, M, f_i, \Delta f$, etc.) as those used for Figs. 5(a) and (b). The results are shown in Table 1. Besides, the results of the AUT measurement are also shown in the table (see also Figs. 5(a) and (b)). From the table, we can see that the delay time of the main path signal for the STD is longer by 1-2 nsec than that for the AUT. The AUT (monopole) and the aperture of the STD (horn) were placed at the same position in our experiment. The feed point of the STD is slightly far from the aperture. Thus, the delay time for the STD is longer than that for the AUT. Also, as we stated previously, the signal parameters ($s_i; i=1, 2, \dots, d$) were assumed to be frequency invariant through the used frequency band for the MUSIC algorithm.

Here, we compare the estimated results by the MUSIC algorithm with those by the FFT-GATE. In Table 1, we show also the estimated values by the FFT-GATE at frequency 3.018 GHz. They were obtained by the 1 GHz bandwidth data whose time-domain response is shown in Fig. 4 (marked by "1 GHz span"). 3.018 GHz is the center of the frequency band 3-3.036 GHz which was used for the MUSIC-MSSP ($M=6$). From Table 1, we can see that the estimated values by the MUSIC algorithm are coinci-

Table 1 Estimated values by the MUSIC algorithm and FFT. The values marked by * denote the estimated values at frequency of 3.018 GHz.

TECHNIQUE	BANDWIDTH(MHz)	AUT			STD		G^{AUT} (dB)
		t_1 (nsec)	t_2 (nsec)	$ s_1 $ (dB)	t_1 (nsec)	$ s_1 $ (dB)	
FFT-GATE	1000	131.865	139.876	-18.13*	133.810	-1.49*	-0.79*
MUSIC-SSP	(M=1)	not resolved	not resolved	—	133.891	-1.34	—
	(M=2)	131.908	140.562	-17.99	133.894	-1.33	-0.79
	(M=4)	131.952	140.426	-17.92	133.902	-1.31	-0.75
	(M=6)	131.944	140.192	-17.92	133.911	-1.29	-0.76
	(M=8)	131.914	139.938	-17.95	133.919	-1.28	-0.80
MUSIC-MSSP	(M=1)	132.136	140.012	-17.68	133.805	-1.49	-0.36
	(M=4)	131.982	139.770	-17.77	133.391	-1.46	-0.46
	(M=5)	131.788	140.338	-18.10	133.233	-1.45	-0.81
	(M=6)	131.764	140.392	-18.13	132.993	-1.45	-0.84
	(M=8)	131.816	140.208	-18.04	132.781	-1.44	-0.76

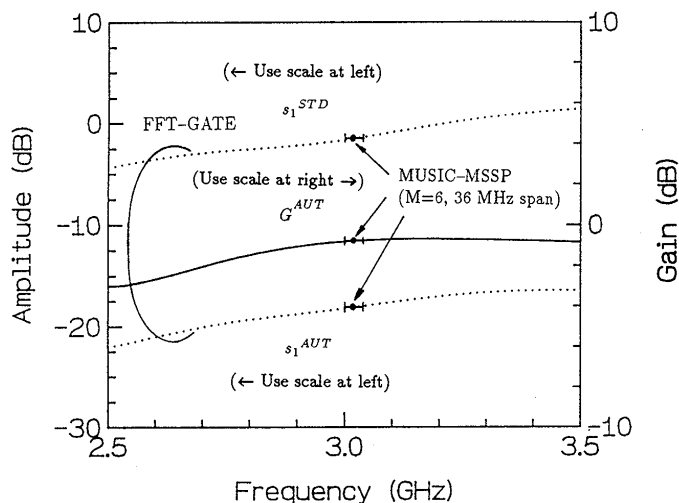


Fig. 8 Estimated main path responses of the AUT and STD, and obtained gain of the AUT.

dent with those values by the FFT-GATE. The discrepancy of the estimated gain (G^{AUT}) between the MUSIC and FFT-GATE is within 0.05 dB except for the MUSIC-MSSP, $M=1$ and 4. Generally, as ' M ' increases, the signal coherence can be destroyed effectively, then the signal detection capability of the MUSIC is improved. This improvement can be seen in the estimated results of the delay times (t_1 and t_2) by the MUSIC-SSP. However, the improvement is not clear for the estimated delay times by the MUSIC-MSSP. This is because the effective decorrelation coefficient is not related to ' M ' monotonically in this preprocessing,⁽⁹⁾ and the decorrelation effect does not affect the eigenvalue distributions as seen from Fig. 6(b). For the signal parameter estimation, we can say that magnitude of the signals estimated by Eq. (12) is not too sensitive to the bias of each estimated delay time though the precise delay time estimation is required for the phase estimation of them. As a result, accuracy improvement of the estimated signal parameter (s_i), also gain, due to the increase of M is not seen clearly from this table.

Also, these results are illustrated in Fig. 8. The results obtained by the MUSIC-MSSP ($M=6$), which are marked by "MUSIC-MSSP ($M=6$, 36 MHz span)," are shown by the notation \cdot . Frequency band which was used for the estimation is shown by the markers $\vdash \dashv$. From this figure, we can see that s_1^{STD} , s_1^{AUT} and G^{AUT} estimated by the MUSIC algorithm coincide with those by the FFT-GATE. The frequency bandwidth required by the MUSIC-MSSP ($M=6$) is only 36 MHz, which is almost 1/28 of that by the FFT-GATE. Note that the gain of the AUT (monopole) was low in our experiment because the ground plane of the monopole antenna was small, and because it was not matched to the feed line well.

From these results, we can say that the MUSIC is useful for elimination of the unwanted signals by

narrow frequency bandwidth data in the antenna measurements. The experiment considered here was the simplest multipath model. However, we can straight-forwardly expand the above procedures for more complicated multipath models as discussed in Sect. 2.

5. Conclusions

In this paper, we have proposed the superresolution technique for the antenna gain measurement, and have shown its availability through the model experiment in the radio anechoic chamber. The interference rejection capability of this method may be also effective for antenna pattern measurements in a multipath environment. In this experiment, the delay time difference between the main and reflected signals is about 8 nsec, then the reflected signal can be regarded as a closely spaced interference. Generally, in the outdoor far-field ranges, the delay time difference of them is expected to be much longer than this experiment, so that the MUSIC algorithm can be expected to work well in much narrower bandwidth. Bias of the estimated parameters (delay time, amplitude and phase of the signals) and resolution capabilities for various kinds of antennas in some typical multipath environments, are the subject to be considered. The measurement error also affects the resolution of the method. Especially, accuracy and stability of an oscillator relate to the mode vector errors in the time domain scanning. This corresponds to the array calibration problem in the direction finding scheme. Systematic studies have not been done on the effect of measurement error to the MUSIC algorithm. They should be done in future. However, we can say that this technique is a promising one to be utilized for antenna measurements in a multipath environment.

References

- (1) Schmidt, R. O., "Multiple emitter location and signal parameter estimation," *IEEE Trans. Antennas & Propag.*, vol. AP-34, no. 3, pp. 276-280, Mar. 1986.
- (2) Shan, T. J., Wax, M. and Kailath, T., "On spatial smoothing for direction-of-arrival estimation of coherent signals," *IEEE Trans. Acoust., Speech & Signal Process.*, vol. ASSP-33, no. 8, pp. 806-811, Aug. 1985.
- (3) Williams, R. T., Prasad, S., Mahalanabis, A. K. and Sibul, L. H., "An improved spatial smoothing technique for bearing estimation in a multipath environment," *IEEE Trans. Acoust., Speech & Signal Process.*, vol. 36, no. 4, pp. 425-432, Apr. 1988.
- (4) Pillai, S. U. and Kwon, B. H., "Forward/Backward spatial smoothing techniques for coherent signal identification," *IEEE Trans. Acoust., Speech & Signal Process.*, vol. 37, no. 1, pp. 8-15, Jan. 1989.
- (5) Briggs, W., "Analyzer improvements make real-time antenna tests practical," *MSN & CT*, pp. 74-86, May 1987.
- (6) Boyles, J. W., "Long range antenna measurements with

the HP8510B using harmonic mixers," *Antenna Measur. Tech. Assoc., Eighth Annu. Meet. and Symp.*, pp. 19-24, Sep. 1986.

- (7) Tufts, D. W. and Kumaresan, R., "Estimation of frequencies of multiple sinusoids: Making linear prediction perform like maximum likelihood," *Proc. IEEE*, vol. 70, no. 9, pp. 975-989, Sep. 1982.
- (8) Roy, R. and Kailath, T., "ESPRIT-Estimation of signal parameters via rotational invariance techniques," *IEEE Trans. Acoust., Speech & Signal Process.*, vol. 37, no. 7, pp. 984-995, Jul. 1989.
- (9) Yamada, H., Ohmiya, M., Ogawa, Y. and Itoh, K., "Superresolution techniques for time-domain measurements with a network analyzer," *IEEE Trans. Antennas & Propag.*, vol. 39, no. 2, pp. 177-183, Feb. 1991.
- (10) Evans, G. E., *Antenna Measurement Techniques*, Boston: MA, Artech House, 1990.
- (11) Munier, J. and Delisle, G. Y., "Spatial analysis in passive listening using adaptive techniques," *Proc. IEEE*, vol. 75, no. 11, pp. 1458-1471, Nov. 1987.



Kiyohiko Itoh was born in Sapporo, Japan, on May 15, 1939. He received the B.S.E.E., M.S., and Ph.D. degrees from Hokkaido University, Sapporo, Japan, in 1963, 1965, and 1973, respectively. Since 1965, he has been on the faculty of Engineering at Hokkaido University, where he is currently a Professor of Electronic Engineering. During 1970-1971, he was with the Department of Electrical and Computer Engineering, Syracuse University, Syracuse, NY, as a Research Associate, on leave from Hokkaido University. His special interests are in electromagnetic radiation, superresolution techniques, mobile radio communications, and solar power satellites. He received SPS91 award in 1991. Dr. Itoh is a member of the IEEE and the Institute of Television Engineering of Japan.



Hiroyoshi Yamada was born in Obihiro, Japan, on November 2, 1965. He received the B.S., M.S., and degrees from Hokkaido University, Sapporo, Japan, in 1988, 1990, and 1993, respectively, both in electronic engineering. He has been a Research Associate at Niigata University since 1993. His current research involves superresolution techniques, electromagnetic wave measurements, and signal processings.



Yasutaka Ogawa was born in Sapporo, Japan, on March 22, 1950. He received the B.S., M.S., and Ph.D. degrees from Hokkaido University, Sapporo, Japan, in 1973, 1975, and 1978, respectively. Since 1979, he has been with Hokkaido University, where he is currently an Associate Professor of Electronic Engineering. Since 1992, he has been with ElectroScience Laboratory, the Ohio State University, Columbus, OH, as a

Visiting Scholar, on leave from Hokkaido University. His special interests are in superresolution techniques, adaptive array antennas, and digital communication systems. Dr. Ogawa is a member of the IEEE.